Columnar and smectic order in binary mixtures of aligned hard cylinders

Shi-Min Cui*
Department of Physics, University of Waterloo, Waterloo, Ontario, Canada N2L 3G1

Zheng Yu Chen
Guelph-Waterloo Program for Graduate Work in Physics and Department of Physics, University of Waterloo, Waterloo, Ontario, Canada N2L 3G1

(Received 7 March 1994)

We examine possible nematic to smectic and nematic to columnar phase transitions for binary mixtures of perfectly parallel aligned hard cylinders with equal diameters but different lengths by using the free-energy functional within the third virial coefficient approximation. The regions of stability are located and the phase diagram of the system is calculated for different values of the ratio of the two cylindrical lengths. The nematic phase can directly transform into the columnar phase for values with a length ratio smaller than 0.635, showing that dispersity in molecular length can stabilize columnar versus smectic ordering of these mixtures.

PACS number(s): 64.70.Md, 61.30.Cz, 61.41.+e

I. INTRODUCTION

The system of monodisperse hard rods is a simple model that is used extensively in both theoretical calculations and computer simulations to represent the molecules comprising liquid-crystalline materials [1]. Traditionally, the structures of liquid-crystalline states are categorized according to the properties of the orientational and spatial order of the molecules [2]. The evidence that hard-core repulsions between rigid-rod molecules play an important role in the formation of orientational order was furnished originally by the Onsager theory [3], and has since been shown by many theoretical and experimental studies [4]. It has also been demonstrated that for monodisperse hard rods the effects of excluded volume interactions associated with the ends of the rodlike molecules can balance out translational entropy effects, thereby stabilizing smectic-A (Sm-A) order [5–7]. A recent Monto Carlo (MC) simulation of binary mixtures of hard spherocylinders with different lengths has further shown that a nematic-columnar transition is possible for sufficiently large length ratios [8]. This is an interesting observation, since in several examples highly concentrated bipolymer solutions exhibit a stable columnar (C) phase [9–11].

In this paper, we analyze the formation of spatially ordered liquid-crystalline phases using the systematic virial expansion of the excess free-energy functional for a binary system composed of aligned hard, right circular cylinders with the same diameter D but different lengths L_1 and L_2. The Onsager theory established that for very thin rigid-rod particles the isotropic-nematic transition occurs at very low volume fraction, and the virial expansion may be truncated after the second virial term, leading to an exact theory for infinitely thin particles [1,3]. The dimensional arguments used by Onsager [3] and others [5,6] make it clear that phase transitions between mesophases in hard-rod systems, such as the nematic–smectic-A transition, occur at high densities just below the close packing density even for thin particles. The low density second-virial approximation is no longer accurate. Since all virial terms are of same order for closely packed rods, more terms should be required in the free-energy expansion. In practice, however, the calculation of the virial terms beyond the fourth order term is extremely difficult; one usually resorts to using complicated diagrammatic-expansion techniques [5]. Mulder [5], in his studies of the nematic-smectic transition for monodisperse hard parallel cylinders, takes into account the third- and fourth-order terms and locates the transition by a bifurcation analysis, which gives a result in good agreement with computer simulations [7,12]. The addition of the third-order term to the free energy gives significant improvement on the bifurcation density for monodisperse hard parallel cylinders [5] and spherocylinders [6]. However, the addition of the fourth-order term gives only a small correction [5]. In the following, we generalize the method of free-energy virial expansion of Mulder to investigate binary mixtures of hard parallel cylinders. The virial expansion, truncated after the third-order term, is used to determine the nematic-smectic and nematic-columnar phase transitions.

In this paper, the stabilities of the smectic and columnar phases are examined. A number of other complications are not considered in our analysis. First, when the number density increases, it is presumed that several solid phases can be established [2,7,12]. This phenomenon is taken into account in the MC analysis for the binary mixture of perfectly aligned hard spherocylinders [8]; we are not aware of any analytic calculation that accounts for these solid phases. Second, the possibility that the spatially ordered liquid-crystalline structure may have modulated states other than the Sm-A or C states is not examined. For instance, the smectic-C struc-

*Permanent address: Department of Applied Physics, Jiao Tong University, Shanghai 200030, People's Republic of China.

ture exists widely in other liquid-crystal materials. In principle, the free energy should be minimized subject to all possible modulated structures. Finally, we have used cylindrical molecules in our calculation, while Stroobants has used spherocylinders in his MC analysis [8]. The shape difference of these two types of molecules may result in different phase behavior. It is therefore desirable to perform a MC simulation for hard cylinders in the same regime of the phase diagram that interests us here. A similar calculation of the present model for hard spherocylinders would require much more work [6].

II. BASIC FORMALISM

A. Free energy

The phase transitions between the nematic state and a spatially ordered liquid-crystalline state, such as the smectic or columnar state considered here, are driven from a competition between the translational entropy and intermolecular interactions favoring spatial ordering. In comparison, the isotropic-nematic phase transition is induced when the excluded-volume interaction, which favors orientational order, becomes more important than the orientational entropy term in the free energy. Owing to the high degree of orientational ordering in Sm-A and C states, it should suffice to represent the molecules by perfectly aligned ones. Such a simplification enables us to write the number density distribution, which otherwise is a function of coupled variables Ω and $\mathbf{r}$, as a product of a δ-function distribution for the orientational degree of freedom, and a spatial modulation function for spatial ordering. Based on this treatment, the free energy can be obtained according to the standard theory of classical fluids.

Consider the system of a binary mixture of perfectly aligned hard cylindrical molecules with different lengths L_1 and L_2 but the same diameters D. The free energy of this system with volume V can therefore be treated as a functional of the number density distribution functions $\rho_\sigma(\mathbf{r})$, where σ labels cylinders of type $\sigma(=1,2)$, respectively. Choosing the z axis as the orientational-alignment direction, we can write the free energy F, scaled by the Boltzmann factor $\beta=(kT)^{-1}$, as a sum of the ideal-gas contribution βF^{ideal} and the nth-order virial coefficient terms E_n [13]:

$$\beta F[\rho_1,\rho_2]=\beta F^{\text{ideal}}[\rho_1,\rho_2]-E_2[\rho_1,\rho_2]-E_3[\rho_1,\rho_2]-\cdots , \tag{1}$$

where

$$\beta F^{\text{ideal}}[\rho_1(\mathbf{r}),\rho_2(\mathbf{r})]=\sum_{\sigma=1,2}\int d\mathbf{r}\,\rho_\sigma(\mathbf{r})[\ln\lambda_\sigma^3\rho_\sigma(\mathbf{r})-1] , \tag{2}$$

with λ_σ being the thermal de Broglie wavelength, and

$$E_2[\rho_1(\mathbf{r}),\rho_2(\mathbf{r})]=\frac{1}{2V}\sum_{\sigma_1\sigma_2}\int d\mathbf{r}_1 d\mathbf{r}_2 f_{\sigma_1\sigma_2}(\mathbf{r}_1-\mathbf{r}_2)\rho_{\sigma_1}(\mathbf{r}_1)\rho_{\sigma_2}(\mathbf{r}_2) , \tag{3}$$

$$E_3[\rho_1(\mathbf{r}),\rho_2(\mathbf{r})]=\frac{1}{6V}\sum_{\sigma_1\sigma_2\sigma_3}\int d\mathbf{r}_1 d\mathbf{r}_2 d\mathbf{r}_3 f_{\sigma_1\sigma_2}(\mathbf{r}_1-\mathbf{r}_2)f_{\sigma_2\sigma_3}(\mathbf{r}_2-\mathbf{r}_3)f_{\sigma_3\sigma_1}(\mathbf{r}_3-\mathbf{r}_1)\rho_{\sigma_1}(\mathbf{r}_1)\rho_{\sigma_2}(\mathbf{r}_2)\rho_{\sigma_3}(\mathbf{r}_3) . \tag{4}$$

In the latter expressions, $f_{\sigma\sigma'}$ stands for the Mayer function for aligned hard cylinders:

$$f_{\sigma\sigma'}(\mathbf{r})=-\Theta(D^2-x^2-y^2)\Theta(L_{\sigma\sigma'}-|z|) \quad (\sigma,\sigma'=1,2) , \tag{5}$$

where Θ is the Heaviside step function, and

$$L_{\sigma\sigma'}=(L_\sigma+L_{\sigma'})/2 . \tag{6}$$

The virial coefficient terms in Eqs. (3) and (4) are related to the sum of all connected irreducible diagrams with n black ρ_σ circles and $f_{\sigma\sigma'}$ bonds. Expressions of the virial coefficients for spatially modulated one-component hard cylindrical molecules (capped and uncapped) can be found in Refs. [5,6].

B. The stability of the nematic phase

In this section we obtain a general expression for the static structure function $S(\mathbf{q})$ by considering Sm-A and C perturbations from a nematic state, which is useful in exploring the stability of the nematic phase. For this purpose, we introduce the Fourier transformations of the number density functions,

$$\rho_\sigma(\mathbf{r})=\sum_{\mathbf{q}}\bar{\rho}_\sigma(\mathbf{q})\exp(i\mathbf{q}\cdot\mathbf{r}) \quad (\sigma=1,2) , \tag{7}$$

where $\bar{\rho}_\sigma$ are coefficients of the different Fourier modes, obeying the relation

$$\bar{\rho}_\sigma^*(\mathbf{q})=\bar{\rho}_\sigma(-\mathbf{q}) . \tag{8}$$

Note that the average number density over one period, ρ_σ, is related to the coefficient of the zeroth mode:

$$\rho_\sigma=\bar{\rho}_\sigma(0) .$$

To quadratic order in $\bar{\rho}_\sigma(\mathbf{q})$, the free energy can be written as

$$\beta\Delta F=\beta F-\beta F^{\text{nematic}}$$

$$=\tfrac{1}{4}\sum_{\sigma_1,\sigma_2}\sum_{\mathbf{q}}\bar{\rho}_{\sigma_1}(\mathbf{q})\bar{\rho}_{\sigma_2}^*(\mathbf{q})A_{\sigma_1\sigma_2}(\mathbf{q})+\cdots , \tag{9}$$

where $A_{\sigma_1\sigma_2}$ is the element of the marix

$$A(\mathbf{q})=S^{-1}(\mathbf{q})=\begin{bmatrix} 1-\rho_1 C_{11}(\mathbf{q}) & -\sqrt{\rho_1\rho_2}C_{12}(\mathbf{q}) \\ -\sqrt{\rho_1\rho_2}C_{21}(\mathbf{q}) & 1-\rho_2 C_{22}(\mathbf{q}) \end{bmatrix}, \tag{10}$$

with $C_{\sigma_1\sigma_2}$ being the Fourier transformation of the direct correlation function [14] obtained from the virial terms in (1).

The onset of a stable modulated phase with wave vector $\mathbf{q}$ is signaled by the bifurcation condition

$$\det[A(\mathbf{q})]=0 . \tag{11}$$

In general, for a mixture of two different types of molecules, such an equation has two possible roots for a given $\mathbf{q}$, which correspond to the condition $\lambda(\mathbf{q})=0$ and $\lambda'(\mathbf{q})=0$, respectively, where $\lambda(\mathbf{q})$ and $\lambda'(\mathbf{q})$ are two eigenvalues of the matrix in (10). Throughout this paper, we assume that $\lambda(\mathbf{q})$ is always the smaller eigenvalue of (10) so that the stability limit is determined by $\lambda(\mathbf{q})=0$ for a given $\mathbf{q}$; any complications caused by the $\lambda'(\mathbf{q})$ mode are neglected.

For later convenience, we introduce a dimensionless average density

$$\eta_\sigma=\tfrac{1}{4}\pi D^2 L_\sigma \rho_\sigma \quad (\sigma=1,2) , \tag{12}$$

corresponding to the packing fraction of type-σ molecules, and scaled wave numbers $Q_\perp=q_\perp D$ and $Q_\parallel=q_\parallel \bar{L}$ with $\bar{L}=\frac{1}{2}(L_1+L_2)$ being the average length. The difference in lengths is represented by the ratio

$$\alpha=L_1/\bar{L}=\frac{2L_1}{L_1+L_2} , \tag{13}$$

which serves as a parameter to characterize the difference in the two types of molecules. Note that $\alpha=0$ is the limit $L_1=0$ and $\alpha=1$ is the limit $L_1=L_2$. Our main interest is in those systems with $0\le\alpha\le 1$.

In the following, we shall investigate possible N–Sm-A and N-C transitions using the bifurcation condition. The Sm-A modulation is associated with longitudinal bifurcation wave vectors $\mathbf{q}^{\text{Sm-}A}=q_\parallel\mathbf{k}$ and $-\mathbf{q}^{\text{Sm-}A}$. Equation (7) for $\rho_\sigma(\mathbf{r})$ therefore becomes

$$\rho_\sigma(\mathbf{r})=\rho_\sigma+2|\bar{\rho}_{\sigma,1}|\cos(q_\parallel z+\varphi_{\sigma,1}) \quad (\sigma=1,2) , \tag{14}$$

where we have written $\bar{\rho}_\sigma(\mathbf{q}^{\text{Sm-}A})=|\bar{\rho}_{\sigma,1}|\exp(i\varphi_{\sigma,1})$. Higher-order harmonic contributions to (14) are not important for the bifurcation analysis and are thus neglected.

The C modulation is characterized by the transverse wave vectors

$$\mathbf{q}_1^C=q_\perp\mathbf{i} ,$$

$$\mathbf{q}_2^C=-\frac{1}{2}q_\perp\mathbf{i}+\frac{\sqrt{3}}{2}q_\perp\mathbf{j} ,$$

$$\mathbf{q}_3^C=-\frac{1}{2}q_\perp\mathbf{i}-\frac{\sqrt{3}}{2}q_\perp\mathbf{j} ,$$

and $-\mathbf{q}_1^C,-\mathbf{q}_2^C,-\mathbf{q}_3^C$. Therefore $\rho_\sigma(\mathbf{r})$ is modulated in accordance with the two-dimensional hexagonal order

$$\rho_\sigma(\mathbf{r})=\rho_\sigma+2|\bar{\rho}_{\sigma,1}|\sum_{i=1}^{3}\cos(\mathbf{q}_i^C\cdot\mathbf{r}+\varphi_{\sigma,1}) \quad (\sigma=1,2) , \tag{15}$$

where we have used the symmetry conditions of a hexagonal lattice to obtain the same coefficients and phases for different $\mathbf{q}_i^C$.

Using this notation we can write the coefficients $A_{\sigma_1\sigma_2}$ in Eq. (9) as

$$A_{\sigma_1\sigma_2}(\mathbf{q})=\delta_{\sigma_1\sigma_2}-\sqrt{\rho_{\sigma_1}\rho_{\sigma_2}}\left[\int d\mathbf{r}\, f_{\sigma_1\sigma_2}(\mathbf{r})\cos(\mathbf{q}\cdot\mathbf{r})+\int d\mathbf{r}\int d\mathbf{r}'\sum_{\sigma_3}\rho_{\sigma_3}f_{\sigma_1\sigma_2}(\mathbf{r})f_{\sigma_2\sigma_3}(\mathbf{r}')f_{\sigma_3\sigma_1}(\mathbf{r}-\mathbf{r}')\cos(\mathbf{q}\cdot\mathbf{r})\right] . \tag{16}$$

The explicit expressions for $\mathbf{q}=\mathbf{q}^{\text{Sm-}A},\mathbf{q}^C$ can be found in Appendix A.

In order to determine the relative phase $\varphi_{\sigma,1}$ of the Fourier components $\bar{\rho}_\sigma$, we minimize F with respect to $\varphi_{\sigma,1}$, which leads to the phase difference $\varphi_{2,1}-\varphi_{1,1}=\pi$. By making use of the above result, we can absorb these phases into order parameters by rescaling the order parameters as $\phi_{\sigma,1}(\mathbf{q})\sim\bar{\rho}_{\sigma,1}(\mathbf{q})\cos(\varphi_{\sigma,1})$.

Summarized briefly, the loss of stability of the nematic phase is determined by

$$\begin{vmatrix} A_{11} & A_{12} \\ A_{21} & A_{22} \end{vmatrix}=0 , \tag{17}$$

and

$$\frac{\partial}{\partial Q}\begin{vmatrix} A_{11} & A_{12} \\ A_{21} & A_{22} \end{vmatrix}=0 . \tag{18}$$

Solving these two equations yields the stability limit $\eta_1(Q)$ and $\eta_2(Q)$ for a given Q, since $A_{\sigma\sigma'}$ are functions of η_1, η_2, and Q in general.

III. PHASE TRANSITIONS

To locate the N–Sm-A and N-C transitions we must consider the fourth-order Landau expansion of the free-energy difference in the relevant order parameters. For consistency, we retain in the expansion the Fourier coefficients up to the second harmonics. For the Sm-A modulation, the number density $\rho_\sigma(\mathbf{r})$ is given by

$$\rho_\sigma(\mathbf{r})=\rho_\sigma+2|\bar{\rho}_{\sigma,1}|\cos(q_\parallel z+\varphi_{\sigma,1}) +2|\bar{\rho}_{\sigma,2}|\cos(2q_\parallel z+\varphi_{\sigma,2}) \quad (\sigma=1,2) , \tag{19}$$

and for the C modulation,

$$\rho_\sigma(\mathbf{r})=\rho_\sigma+2|\bar{\rho}_{\sigma,1}|\sum_{i=1}^{3}\cos(\mathbf{q}_i^C\cdot\mathbf{r}+\varphi_{\sigma,1}) +2|\bar{\rho}_{\sigma,2}|\sum_{i=4}^{6}\cos(\mathbf{q}_i^C\cdot\mathbf{r}+\varphi_{\sigma,2}) \quad (\sigma=1,2) . \tag{20}$$

In Eq. (20), the three next-shortest reciprocal-lattice vectors, characteristic of the plane hexagonal lattice, are chosen as

$$\mathbf{q}_4^C=\frac{3}{2}q_\perp\mathbf{i}-\frac{\sqrt{3}}{2}q_\perp\mathbf{j} ,$$

$$\mathbf{q}_5^C=-\frac{3}{2}q_\perp\mathbf{i}-\frac{\sqrt{3}}{2}q_\perp\mathbf{j} ,$$

$$\mathbf{q}_6^C=\sqrt{3}q_\perp\mathbf{j} .$$

By using the selection rules and carrying out the integrations in the second and third virial terms, we obtain the fourth-order Landau expansion of the free-energy difference:

$$\frac{\beta\Delta F}{N}=\sum_{\sigma_1\sigma_2}A_{\sigma_1\sigma_2}(Q)\phi_{\sigma_1,1}\phi_{\sigma_2,1} -\frac{2}{c_1}\sum_{\sigma_1\sigma_2\sigma_3}B_{\sigma_1\sigma_2\sigma_3}(Q)\phi_{\sigma_1,1}\phi_{\sigma_2,1}\phi_{\sigma_3,2} +\sum_{\sigma_1\sigma_2}A_{\sigma_1\sigma_2}(c_1Q)\phi_{\sigma_1,2}\phi_{\sigma_2,2} +\sum_\sigma\frac{c_2}{\rho_\sigma}\phi_{\sigma,1}^4+\Delta F^{(3)} , \tag{21}$$

where the cubic invariant term $\Delta F^{(3)}$ is zero for the Sm-A phase,

$$\Delta F^{(3)}=0 , \tag{22a}$$

and nonzero for the C phase

$$\Delta F^{(3)}=-\frac{2}{3\sqrt{3}}\sum_{\sigma_1\sigma_2\sigma_3}B_{\sigma_1\sigma_2\sigma_3}(Q)\phi_{\sigma_1,1}\phi_{\sigma_2,1}\phi_{\sigma_3,1} , \tag{22b}$$

due to $\mathbf{q}_1+\mathbf{q}_2+\mathbf{q}_3=0$ for the C modulation. In Eq. (21) $c_1=2$ (Sm-A), $\sqrt{3}$ (C), and $c_2=\frac{1}{2}$ (Sm-A), $\frac{5}{6}$ (C) are constants from the translational entropy term. The phase $\varphi_{\sigma,2}$ as in the case for the phase $\varphi_{\sigma,1}$, is determined by minimizing the free energy with respect to $\varphi_{\sigma,2}$, which gives the condition $\varphi_{2,2}-\varphi_{1,2}=\pi$. The order parameters $\phi_{\sigma,1}$ and $\phi_{\sigma,2}$ are related to the Fourier coefficients $\bar{\rho}_{\sigma,1}$ and $\bar{\rho}_{\sigma,2}$ in Eqs. (19) and (20) by

$$\phi_{\sigma,n}=\left[\frac{c_1}{\rho_\sigma}\right]^{1/2}|\bar{\rho}_{\sigma,n}|\cos(\varphi_{\sigma,n}) \ (\sigma=1,2,n=1,2) , \tag{23}$$

where we have scaled the order parameter $|\bar{\rho}_{\sigma,n}|$ in a form that will be more convenient in the actual calculations. The coefficients $A_{\sigma\sigma'}(Q)$ can be found in Appendix A, while the coefficients $B_{\sigma_1\sigma_2\sigma_3}(Q)$ can be found in Appendix B.

As explained in the preceding section, the matrix $A_{\sigma\sigma'}$ has two eigenvalues λ and λ', chosen so that $\lambda<\lambda'$. We can assume that the phase behavior is mainly determined by the λ mode since λ' is always positive. Keeping this in mind, we can diagonalize the matrix A through a Hermitian matrix and write

$$\phi_{\sigma,n}=\beta_\sigma(Q)\Phi_n \quad (\sigma=1,2,n=1,2) , \tag{24}$$

where Φ_n are the eigenvectors corresponding to the λ mode. Coefficients $\beta_\sigma(Q)$ and $\lambda(Q)$ can be found in Appendix C.

Using these definitions of coefficients, we finally arrive at the free energy

$$\frac{\beta\Delta F}{N}=\lambda(Q)\Phi_1^2-a(Q)\Phi_1^3+\lambda(c_1Q)\Phi_2^2+\sum_\sigma\frac{c_2\beta_\sigma^4(Q)}{\rho_\sigma}\Phi_1^4 -\frac{2}{c_1}\sum_{\sigma_1\sigma_2\sigma_3}B_{\sigma_1\sigma_2\sigma_3}(Q)\beta_{\sigma_1}(Q)\beta_{\sigma_2}(Q) \times\beta_{\sigma_3}(c_1Q)\Phi_1^2\Phi_2 , \tag{25}$$

with

$$a(Q)=0 \tag{26a}$$

for Sm-A, and

$$a(Q)=\frac{2}{3\sqrt{3}}\sum_{\sigma_1\sigma_2\sigma_3}B_{\sigma_1\sigma_2\sigma_3}(Q)\beta_{\sigma_1}(Q)\beta_{\sigma_2}(Q)\beta_{\sigma_3}(Q) , \tag{26b}$$

for C. Equation (25) is a typical Landau expansion in the order parameters Φ_1 and Φ_2. The latter can be related to the former by minimizing ΔF with respect to Φ_2. Taking $\partial\Delta F/\partial\Phi_2=0$ yields

$$\Phi_2=\frac{1}{c_1\lambda(c_1Q)}\sum_{\sigma_1\sigma_2\sigma_3}B_{\sigma_1\sigma_2\sigma_3}(Q)\beta_{\sigma_1}(Q) \times\beta_{\sigma_2}(Q)\beta_{\sigma_3}(c_1Q)\Phi_1^2 , \tag{27}$$

thus the free energy becomes

$$\frac{\beta\Delta F}{N}=\lambda(Q)\Phi_1^2-a(Q)\Phi_1^3+b(Q)\Phi_1^4 , \tag{28}$$

with

$$b(Q)=\sum_\sigma\frac{c_2\beta_\sigma^4(Q)}{\rho_\sigma} -\frac{1}{c_1^2\lambda(c_1Q)}\left[\sum_{\sigma_1\sigma_2\sigma_3}B_{\sigma_1\sigma_2\sigma_3}(Q)\beta_{\sigma_1}(Q)\beta_{\sigma_2}(Q) \times\beta_{\sigma_3}(c_1Q)\right]^2 . \tag{29}$$

When $a(Q)=0$, as in the case of the N–Sm-A transition, the free energy (28) describes a second-order phase transi-

tion whose phase boundary is directly related to the conditions (17) and (18). When $a(Q)\neq 0$, as in the case of the N-C transition, the free energy (28) describes a first-order phase transition. The stability conditions (17) and (18) only determine the stability limit; the actual phase boundary is fixed by the condition $\Delta F=0$ and $\partial\Delta F/\partial Q=0$, or effectively,

$$\lambda_{\text{eff}}(Q)=0 , \tag{30}$$

and

$$\frac{\partial}{\partial Q}\lambda_{\text{eff}}(Q)=0 , \tag{31}$$

where

$$\lambda_{\text{eff}}(Q)=\lambda(Q)-\frac{a^2(Q)}{4b(Q)} . \tag{32}$$

Based on these procedures, we have studied possible nematic-smectic and nematic-columnar phase transitions. The phase diagrams displayed in Fig. 1 show the regions of stability of the nematic, smectic, and columnar phases. The nematic-smectic transition is continuous and the phase boundary is represented by the dotted curves. The first-order nematic-columnar phase transition is represented by the solid curves in Fig. 1.

For completeness, we have also compared the free energy of the Sm-A and C phases to obtain the first-order Sm-A-C transition boundary. We do not claim that such a comparison will produce the exact phase bound-

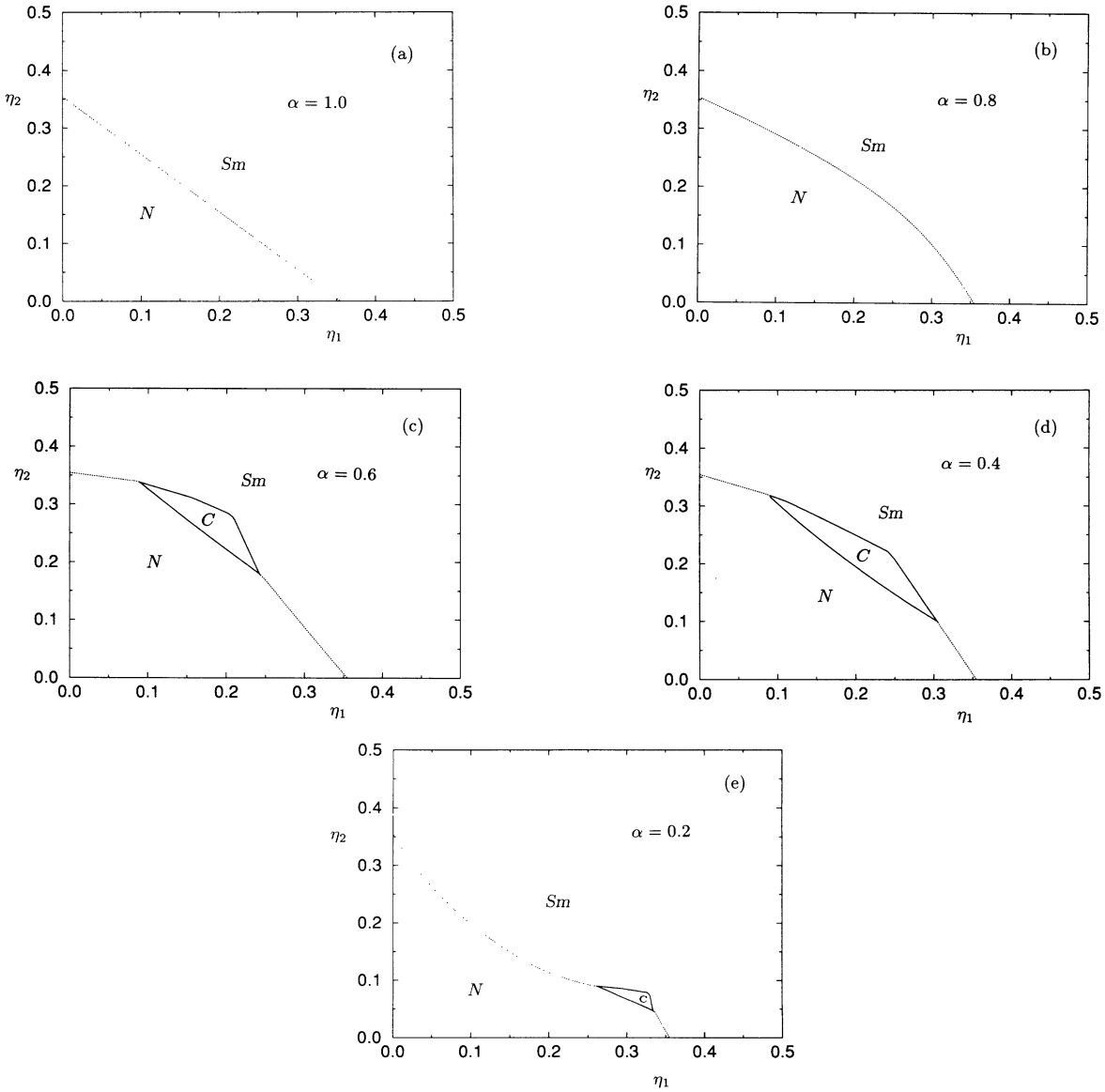

FIG. 1. Phase diagrams in the η_1-η_2 plane for binary mixtures of hard parallel cylinders with the same diameters for $\alpha=1.0$ (a), 0.8 (b), 0.6 (c), 0.4 (d), and 0.2 (e), respectively. Here η_1 and η_2 are the dimensionless average densities defined in Eq. (12), and the ratio $\alpha=2L_1/(L_1+L_2)$ defined in Eq. (13). The solid curves represent the first-order nematic-columnar and smectic-columnar transitions. The dotted curves represent the continuous nematic-smectic transitions.

ary between the Sm-A and C phases; the free-energy expansion (27) may fail to be accurate, since higher-order terms should become important away from the N–Sm-A and N-C stability limits. Nevertheless, this comparison gives us a rough indication of the Sm-A–C phase boundary.

The binary mixtures of hard parallel cylinders exhibit a strongly α-dependent phase behavior which must be attributed to the difference in packing properties between the two kinds of rods. In the limit of $\alpha=1$, the phase behavior follows from the model of monodisperse hard rods. The nematic phase is stable for $\eta=\eta_1+\eta_2<0.357$, while the smectic phase is stable for $\eta>0.357$. There is no region of stability for columnar phases. The calculation shows that the nematic-columnar transition lines are always above that of the nematic-smectic transition for $\alpha<0.777$. It appears that at this point $(\alpha=0.777, L_1/L_2=0.635)$ the nematic phase can directly transform into a columnar phase. The nematic-columnar phase transition is weakly first order because of the small coefficient a in the expansion. The size of the stable columnar region is also α dependent. The columnar phase region becomes wider as α decreases from $\alpha=0.777$, but after $\alpha\sim0.4$ that region becomes narrower as α decreases.

The nematic to columnar transition density exhibits weak α dependence ranging from $\eta_1+\eta_2=0.43$ for $\alpha=0.78$ to $\eta_1+\eta_2\sim0.39$ in the small α limit, while the nematic to smectic transition density exhibits strong α dependence as seen from the five examples given in Fig. 1. A sharp decrease of nematic-smectic transition density occurs for small α.

IV. DISCUSSION

Our simple model system of binary mixture hard parallel cylinders exhibits a particularly interesting phase behavior compared to the corresponding monodisperse systems. On the basis of packing effects due to short-range repulsions, it is shown that the theory, accurate up to the third virial approximation, can be used to study the stability of the nematic phase against smectic and columnar perturbations for binary mixtures of hard rods. The location of the smectic-columnar transition can also be roughly estimated. We are unable to demonstrate that the smectic or the columnar phase is stable with respect to a crystalline solid or a more ordered smectic mesophase, which is beyond the scope of the current work.

In our calculation, the diameters of the two types of cylinders are assumed to be the same. A possible way of checking some of these results experimentally would be to determine the structures of the liquid-crystalline phases of, for example, a binary solution of rigid-rod-type polymer molecules of two different polymerization indices. At present, a direct comparison with computer simulation of binary mixtures of perfectly aligned hard rods is not possible because the only result available is for perfectly aligned hard spherocylinders [8]. It is reasonable that our theoretical phase diagrams are different from that obtained by Stroobants [8] since the latter is for the binary system of *spherocylinders*. However, there is one common characteristic in both models, i.e., the nematic phase can directly transform into the columnar phase for certain values of the length ratio, showing that dispersity in molecular length favors columnar order over smectic order.

In the above calculation, we have let the diameters of the two types of molecules be the same. If the actual experimental system is composed of two different types of molecules, rather than the same type of molecules with different polymerization indices, the effect of the difference in diameter must be examined. We have also performed calculations for a binary mixture of aligned hard cylinders with different diameters but the same length. In this case, the nematic-columnar transition curves are always well above the nematic-smectic ones. The columnar phase is never stable. There is only a direct nematic to smectic phase transition as shown in Fig. 2. This result is very different from those obtained for cases where the two types of cylinders have the same diameters but different lengths.

Since our theory is based upon a model of perfectly aligned hard rods, fluctuations of the direction of rods are completely ignored. Only at extremely large densities is this assumption asymptotically valid. The phase transition densities considered above have large but *finite* values. To what extent the coupling to the orientational degree of freedom would affect the phase transitions from the nematic phase to spatially ordered liquid-crystalline phases is still an unresolved problem even for monodisperse systems [6].

We have also neglected contributions of the fourth- and higher-order virial contributions. As shown in the study of the N–Sm-A phase transition of monodisperse system of rigid rods, these high-order terms also contribute weakly to the free energy of the phase transition. The phase diagrams in Fig. 1 could be affected by these high-order virial contributions. However, it is very difficult to estimate the contribution of these high-order terms for the systems considered in this paper.

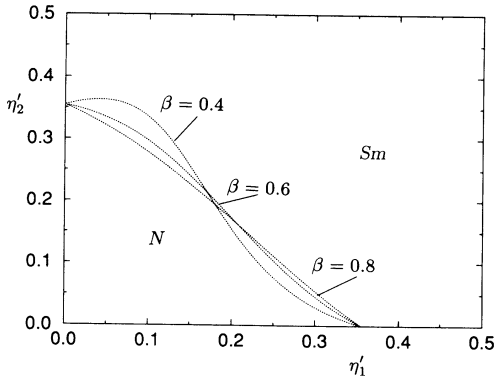

FIG. 2. Phase diagrams in the η_1'-η_2' plane for binary mixtures of hard parallel cylinders with the same lengths but different diameters: $\beta=0.8$, 0.6, and 0.4, respectively. Here the dimensionless average density η_σ' is defined as $\eta_\sigma'=\pi LD_\sigma^2\rho_\sigma/4$ and the parameter β is defined as $\beta=2D_1/(D_1+D_2)$, D_1 and D_2 being the diameters of rigid rods of types 1 and 2, respectively. The dotted curves represent the second-order N-Sm$_-A$ transition.

ACKNOWLEDGMENTS

This work was supported by the National Science and Engineering Research Council of Canada.

APPENDIX A: COEFFICIENT $A_{\sigma_1\sigma_2}$ IN EQS. (17) AND (23)

In this appendix the detailed expressions for $A_{\sigma_1\sigma_2}(\mathbf{q})$ are given. For the Sm-A case,

$$
\begin{aligned}
A_{11}(Q)&=1+8\eta_1[1+4c(\eta_1+\eta_2)]\sin(Q\alpha)/(Q\alpha)+32c\eta_1[\eta_1+\eta_2\alpha/(2-\alpha)][1-\cos(Q\alpha)]/(Q\alpha)^2 ,\\
A_{12}(Q)&=A_{21}(Q)=8\{\eta_1\eta_2/[\alpha(2-\alpha)]\}^{1/2}\\
&\quad\times([1+4c(\eta_1+\eta_2)]\sin Q/Q+4c[\eta_1/\alpha+\eta_2/(2-\alpha)]\{\cos[Q(1-\alpha)]-\cos Q\}/Q^2) ,\\
A_{22}(Q)&=1+8\eta_2[1+4c(\eta_1+\eta_2)]\sin[Q(2-\alpha)]/[Q(2-\alpha)]\\
&\quad+32c\eta_2[\eta_1(2-\alpha)/\alpha+\eta_2]\{1-\cos[Q(2-\alpha)]\}/[Q(2-\alpha)]^2 ,
\end{aligned}
\tag{A1}
$$

with $c=1-3\sqrt{3}/4\pi$ and $Q=q_{\parallel}\bar{L}$. For the C modulations,

$$
\begin{aligned}
A_{11}(Q)&=1+16\eta_1\{J_1(Q)/Q+[3\eta_1+2\eta_2+\eta_2\alpha/(2-\alpha)]c(Q)\} ,\\
A_{12}(Q)&=A_{21}(Q)=\{\eta_1\eta_2/[\alpha(2-\alpha)]\}^{1/2}[\eta_1(4-\alpha)+\eta_2(2+\alpha)]c(Q) ,\\
A_{22}(Q)&=1+16\eta_2\{J_1(Q)+[3\eta_2+2\eta_1+\eta_1(2-\alpha)/\alpha]c(Q)\} ,
\end{aligned}
\tag{A2}
$$

where J_1 is the first-order Bessel function, and

$$
c(Q)=2\int_0^1 r\,dr\,J_0(Qr)\left\{1-\frac{1}{\pi}\left[r\left[1-\frac{r^2}{4}\right]^{1/2}-\cos^{-1}\left[1-\frac{r^2}{2}\right]\right]\right\} .
\tag{A3}
$$

Here $Q=q_{\perp}D$.

APPENDIX B: COEFFICIENT $B_{\sigma_1\sigma_2\sigma_3}$ IN EQ. (23)

In this appendix the detailed expressions for $B_{\sigma_1\sigma_2\sigma_3}(Q)$ are given:

$$
B_{\sigma_1\sigma_2\sigma_3}(Q)=[\delta_{\sigma_1\sigma_2}\delta_{\sigma_1\sigma_3}+C_{\sigma_1\sigma_2\sigma_3}(Q)]/\sqrt{\rho_{\sigma_1}} .
\tag{B1}
$$

For Sm-A

$$
C_{\sigma_1\sigma_2\sigma_3}(Q)=-(\rho_{\sigma_1}\rho_{\sigma_2})^{1/2}\rho_{\sigma_3}\int\int d\mathbf{r}\,d\mathbf{r}'f_{\sigma_1\sigma_2}(\mathbf{r}'-\mathbf{r})f_{\sigma_2\sigma_3}(\mathbf{r})f_{\sigma_3\sigma_1}(\mathbf{r}')\cos[q_{\parallel}(z+z')] ,
\tag{B2}
$$

and the explicit expressions are given by

$$
\begin{aligned}
C_{111}&=32c\eta_1^2[\cos(Q\alpha)-\cos(2Q\alpha)]/[\alpha^2Q^2] ,\\
C_{112}&=32c\eta_1\eta_2\{\cos[Q(2-\alpha)]-\cos(2Q)\}/[\alpha(2-\alpha)Q^2] ,\\
C_{121}&=C_{211}=16c\eta_1^{3/2}\eta_2^{1/2}\{\cos(Q)+\cos[Q(2\alpha-1)]-2\cos[Q(\alpha+1)]\}/[\alpha^{3/2}(2-\alpha)^{1/2}Q^2] ,\\
C_{122}&=C_{212}=16c\eta_2^{1/2}\eta_2^{3/2}\{\cos(Q)+\cos[Q(3-2\alpha)]-2\cos[Q(3-\alpha)]\}/[\alpha^{1/2}(2-\alpha)^{3/2}Q^2] ,\\
C_{221}&=32c\eta_1\eta_2[\cos(Q\alpha)-\cos(2Q)]/[\alpha(2-\alpha)Q^2] ,\\
C_{222}&=32c\eta_2^3\{\cos[Q(2-\alpha)]-\cos[2Q(2-\alpha)]\}/[(2-\alpha)^2Q^2] ,
\end{aligned}
\tag{B3}
$$

with $c=1-3\sqrt{3}/4\pi$. For C,

$$
C_{\sigma_1\sigma_2\sigma_3}(Q)=(\rho_{\sigma_1}\rho_{\sigma_2})^{1/2}\rho_{\sigma_3}\int\int d\mathbf{r}\,d\mathbf{r}'f_{\sigma_1\sigma_2}(\mathbf{r}'-\mathbf{r})f_{\sigma_2\sigma_3}(\mathbf{r})f_{\sigma_3\sigma_1}(\mathbf{r}')\cos(\mathbf{q}_1^C\cdot\mathbf{r}+\mathbf{q}_2^C\cdot\mathbf{r}') ,
\tag{B4}
$$

and the explicit expressions are given by

$$
\begin{aligned}
C_{111} &= 48\eta_1^2 c(Q) , \\
C_{112} &= 16\eta_1\eta_2(4-\alpha)c(Q)/(2-\alpha) , \\
C_{121} &= C_{211} = 16\eta_1^{3/2}\eta_2^{1/2}(4-\alpha)c(Q)/[\alpha(2-\alpha)]^{1/2} , \\
C_{122} &= C_{212} = 16\eta_1^{1/2}\eta_2^{3/2}(2+\alpha)c(Q)/[\alpha(2-\alpha)]^{1/2} , \\
C_{221} &= 16\eta_1\eta_2(2+\alpha)c(Q)/\alpha , \\
C_{222} &= 48\eta_2^2 c(Q) ,
\end{aligned}
\tag{B5}
$$

with

$$
\begin{aligned}
c(Q) = \int_0^1 r\,dr\,J_0(Qr) \Bigg\{ 1 - \frac{1}{\pi} \Bigg[r \left[1 - \frac{r^2}{4} \right]^{1/2} - \cos^{-1} \left[1 - \frac{r^2}{2} \right] + \frac{6}{Q} J_1(Q) \cos^{-1} \frac{r}{2} \Bigg] \\
+ \frac{6}{\pi Q} \int_{\cos^{-1}(r/2)}^{\pi} d\theta [r\cos\theta + (1 - r^2\sin^2\theta)^{1/2}] J_1\{Q[r\cos\theta + (1 - r^2\sin^2\theta)^{1/2}]\} \Bigg\} ,
\end{aligned}
\tag{B6}
$$

where J_0 and J_1 denote the zero- and the first-order Bessel function, respectively.

APPENDIX C: COEFFICIENTS β_1, β_2, AND λ IN EQ. (26)

The explicit expressions for the coefficients $\beta_1(Q)$, $\beta_2(Q)$, and $\lambda(Q)$ are given by

$$
\beta_1(Q) = A_{12}(Q)/\{ A_{12}(Q)A_{21}(Q) + [\lambda(Q) - A_{11}(Q)]^2 \}^{1/2} ,
\tag{C1}
$$

$$
\beta_2(Q) = [\lambda(Q) - A_{11}(Q)]/\{ A_{12}(Q)A_{21}(Q) + [\lambda(Q) - A_{11}(Q)]^2 \}^{1/2} ,
\tag{C2}
$$

$$
\lambda(Q) = (A_{11}(Q) + A_{12}(Q) - \{ [A_{11}(Q) - A_{22}(Q)]^2 + 4A_{12}(Q)A_{21}(Q) \}^{1/2})/2 .
\tag{C3}
$$

[1] G. J. Vroege and H. N. W. Lekkerkerker, Rep. Prog. Phys. **55**, 1241 (1992).

[2] See, e.g., *Polymer Liquid Crystals*, edited by A. Ciferri, W. R. Krigbaum, and R. B. Meyer (Academic, New York, 1982).

[3] L. Onsager, Ann. N.Y. Acad. Sci. **51**, 627 (1949).

[4] See, e.g., R. F. Kayser and H. J. Raveché, Phys. Rev. A **17**, 2067 (1978); T. J. Sluckin and P. Shukla, J. Phys. A **16**, 1539 (1983); M. Baus, J. L. Colot, X. G. Wu, and H. Xu, Phys. Rev. Lett. **59**, 2184 (1987); J. F. Marko, *ibid.* **60**, 325 (1988).

[5] B. Mulder, Phys. Rev. A **35**, 3095 (1987).

[6] A. Poniewierski, Phys. Rev. A **45**, 5605 (1992).

[7] A. Stroobants, H. N. W. Lekkerkerker, and D. Frenkel, Phys. Rev. Lett. **57**, 1452 (1986); Phys. Rev. A **36**, 2929 (1987).

[8] A. Stroobants, Phys. Rev. Lett. **69**, 2388 (1992).

[9] F. Livolant and Y. Bouligand, J. Phys. (Paris) **47**, 1813 (1986).

[10] F. Livolant, A. M. Levelut, J. Doucet, and J. P. Benoit, Nature (London) **339**, 724 (1989).

[11] S.-D. Lee and R. B. Meyer, Liq. Cryst. **7**, 451 (1990).

[12] D. Frenkel, B. M. Mulder, and J. P. McTague, Phys. Rev. Lett. **52**, 287 (1984); D. Frenkel, J. Phys. Chem. **91**, 4912 (1987); **92**, 3280 (1988); J. A. C. Veerman and D. Frenkel, Phys. Rev. A **41**, 3237 (1990).

[13] G. Stell, in *The Equilibrium Theory of Classical Fluids*, edited by H. F. Frisch and J. L. Lebowitz (Benjamin, New York, 1964).

[14] J. Percus, in Ref. [13].